NASA
Technical Memorandum 105717

AVSCOM
Technical Report 92–C–026

P.8

A 4-Spot Time-of-Flight Anemometer for Small Centrifugal Compressor Velocity Measurements

Mark P. Wernet
Lewis Research Center
Cleveland, Ohio

and

Gary J. Skoch
Propulsion Directorate
U.S. Army Aviation Systems Command
Lewis Research Center
Cleveland, Ohio

Prepared for the
Sixth International Symposium on the Application of Laser Techniques to Fluid Mechanics
sponsored by the Instituto Superio Téchico
Lisbon, Portugal, July 20–23, 1992

NASA

US ARMY AVIATION SYSTEMS COMMAND

spacing to spot diameter (width) is decreased to increase the effective acceptance angle. Increasing the elliptical spot height, however, compromises the laser light flux in the probe volume. The illuminated region is still small compared to fringe systems, and hence still provides for superior stray light discrimination. Classic 2-Spot systems have a high light flux through the probe volume, typically 2-3 orders of magnitude larger than a comparable fringe system (Schodl 1986). An elliptical 2-Spot system has a lower light flux than the classic 2-Spot system, reduced only by the ratio of the ellipse height to the width (assuming the elliptical spot width is equal to the circular spot diameter). An elliptical 4-Spot system would decrease the light flux by another factor of 2. For the 4-Spot system described here, the light flux in the probe volume is an order of magnitude larger than a comparable fringe system and an order of magnitude smaller than a classic 2-Spot.

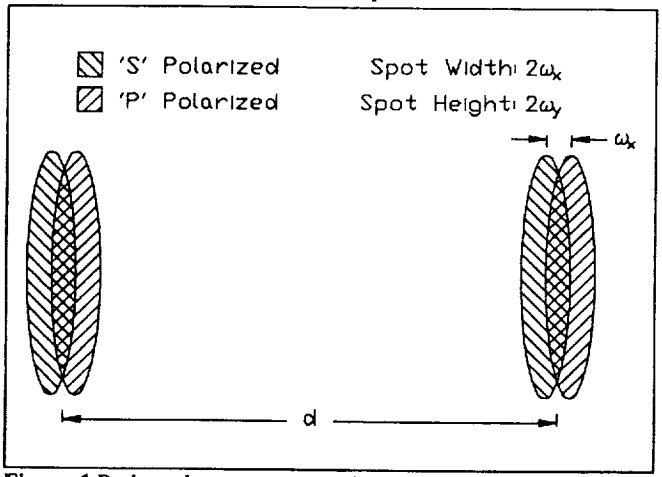

Figure 1 Probe volume geometry, showing orthogonally polarized, overlapping elliptical spot pairs.

The processing of the unipolar TOFA signals is not a simple task. Lading (1983) also analyzed the optimal processing strategy for estimating the transit time of a particle through the probe volume. As estimating the zero-cross time of a bipolar signal would be a simpler task than estimating the peak position of a photodetected signal, Lading (1983) proposed a spatial lead-lag operator to provide optimally shaped bipolar pulses. Hence, the signal processing requirements would be substantially relaxed. Part of the signal processing, the generation of a bipolar pulse from a unipolar pulse, would be done optically before photon detection. The lead-lag operator could be implemented by using two partially overlapping, orthogonally polarized spots in the measurement region, see figure 1.

The 2-color, 4-Spot laser anemometer is a single component time-of-flight anemometer following the prescription by Lading (1983). The optical configuration and functional layout of the system is shown in figure 2, and was previously discussed by Wernet & Edwards (1986) and Wernet & Oberle (1987). The spot pair separation is 92μm, and the spots are roughly 50μm×10μm at the $1/e^2$ points. Thus, the acceptance angle is approximately ±30°. The 514 and 488nm lines from an argon-ion laser operating at 4 W multiline are used to generate two overlapping spot pairs separated by a distance d. Use of two colors provides a higher light flux in the probe volume, and better cross-talk discrimination in the detector. Previous 2-color 2-Spot systems have been described by Schodl (1989). Beam shaping optics, employing achromatic cylindrical lenses, are used to form an elliptical beam. A Pellin-Broca prism is used to symmetrically disperse the green and blue beams. The orthogonally polarized, partially overlapping spot pairs are generated using a λ/4 waveplate followed by a Wollaston prism. Color and polarization are used to separate the light scattered from particle transits across the probe volume producing two pairs of electronic pulses, each pair overlapping by half of the pulse width. The scattered light is collected through an f/4 200 mm focal length lens L3 and routed onto four PMTs. The overlapping pulses are electronically subtracted to produce two bipolar pulses, whose zero-cross to zero-cross difference corresponds to the particle time-of-flight. Electronic delays are not required. The fixed spatial overlap of the spots in the probe volume generates an optimally delayed set of pulses for electronic subtraction independent of velocity. The single component anemometer is used to obtain 2-D velocity measurements by rotating the probe volume to a selected number of angular orientations and recording velocity probability density functions (pdfs). The probe volume is rotated using a mirrored dove prism image rotator, which is located between lenses L1 and L2. The pdfs obtained at various probe volume orientations are used to compute the velocity vector magnitude and flow angle. A goniometric stage is used to turn the viewing direction ±45° (perpendicular to the plane of the page), thus enabling the selection of various windows along the centrifugal impeller flowpath.

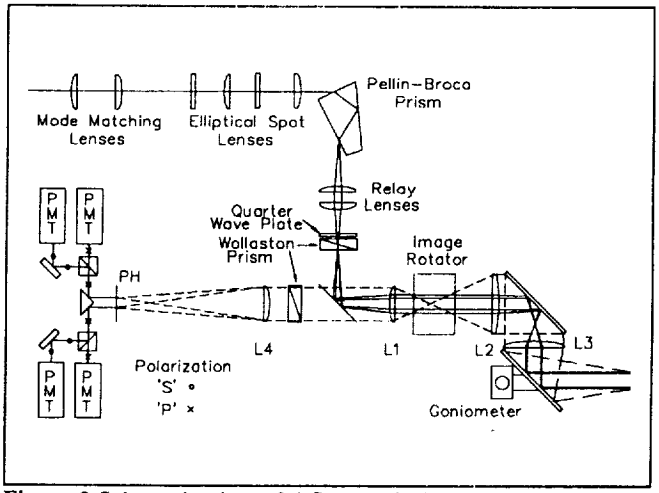

Figure 2 Schematic view of 4-Spot optical components.

Cramer-Rao Lower Bound The 4-Spot TOFA is an optimally configured transit anemometer, employing a spatial lead-lag operator to minimize the measurement error. The detection of light scattered from small particles traversing the probe volume is governed by Poisson statistics. The Cramer-Rao lower bound measurement uncertainty can be employed to determine the limiting accuracy obtainable with TOFA systems (Whalen 1971, Lading 1983), and also to determine the measurement error as a function of the spot overlap (lead-lag delay).

Let the expected number of photoelectron counts in the time interval t_k to $t_k+\Delta t$ be described as a Gaussian signal with a background noise level:

$$\langle N_k \rangle = \frac{P\sigma\Omega\Delta t\eta\lambda}{2\pi\omega_x\omega_y hc}\exp\left\{\frac{-2y_1^2}{\omega_y^2}\right\}\exp\left\{\frac{-2v^2t_k^2}{\omega_x^2}\right\}+\left(\frac{\eta\lambda}{hc}\right)P_n\Delta t \quad (1)$$

where: P is the total laser power in probe volume [2.5 W]
P_n is background noise level [10^{-3} W]
σ is the particle scattering cross section [5×10^{-14} m^2/sr]
Ω is the solid angle of collected light (f/4) [0.05 sr]
ω_x and ω_y are the e^{-2} spot half width and height, respectively [5 and 25 μm]

η is an efficiency factor incorporating photomultiplier quantum efficiency, collection efficiency and other system losses [0.01]

λ is the laser light wavelength [.5 μm]

h is Plank's constant [6.62×10^{-34} J·s]

c is the velocity of light [3×10^{8} m/s]

y_1 is the height above or below the axis the particle traverses the spot [0 μm]

v is the component of the particle velocity along the axis of the spots [100 m/s]

(Quantities in [ ] are sample values used in the analysis below.)

The signal used by the signal processor is the difference of two time shifted Gaussians:

$$\langle N_k\rangle_D = \frac{P\sigma\Omega\Delta t\eta\lambda}{2\pi\omega_x\omega_y hc}\exp\left\{\frac{-2y_1^2}{\omega_y^2}\right\}\times \left[\exp\left\{\frac{-2v^2(t_k-t_z+\tau)^2}{\omega_x^2}\right\}-\exp\left\{\frac{-2v^2(t_k-t_z-\tau)^2}{\omega_x^2}\right\}\right] \quad (2)$$

where τ is the spot lead-lag time [sec], and t_z is the bipolar signal zero-cross time position. Because of the assumption of Poisson statistics, the noise power in the difference signal is given by the sum of the two PMT signals. Assuming that the background noise level in the two signals is the same, the difference signal is:

$$\langle N_k\rangle_N = \frac{P\sigma\Omega\Delta t\eta\lambda}{2\pi\omega_x\omega_y hc}\exp\left\{\frac{-2y_1^2}{\omega_y^2}\right\}\times \left[\exp\left\{\frac{-2v^2(t_k-t_z+\tau)^2}{\omega_x^2}\right\}+\exp\left\{\frac{-2v^2(t_k-t_z-\tau)^2}{\omega_x^2}\right\}\right]+ 2\left(\frac{\eta\lambda}{hc}\right)P_n\Delta t \quad (3)$$

The signal output from the 4-Spot is thus a function of several parameters which can be expressed as the vector:

$$\vec{\alpha} = [t_z, v, \theta, P_n] \quad (4)$$

The Fisher information matrix Γ, for Poisson statistics, is given by (Lading & Jensen 1980):

$$\Gamma_{ij} = \sum_k \frac{1}{\langle N_k\rangle_N}\frac{\partial\langle N_k\rangle_D}{\partial\alpha_i}\frac{\partial\langle N_k\rangle_D}{\partial\alpha_j} \quad (5)$$

where $\langle N_k\rangle_D$ is given by equation 2 and $\langle N_k\rangle_N$ is given by equation 3. If we assume that the parameters are uncorrelated, the Cramer-Rao lower bound measurement uncertainty in the parameter α_i is given by:

$$\sigma_{\alpha_i} = \Gamma_{ii}^{-\frac{1}{2}} \quad (6)$$

The measurement uncertainty in estimating the zero-cross of the bipolar signal is obtained by using $\alpha_i = t_z$. Determining a particle velocity involves estimating two such zero-cross signals. Hence, the error in the measured velocity is then a combination of these two uncertainties. In the 4-Spot processing scheme, only the zero-cross of the bipolar signal is used to estimate the particle transit time. Therefore, we need only evaluate Equation 5 at $t_k=t_z$. For the signal dominated case of a 4-Spot TOFA, the velocity measurement uncertainty is:

$$\frac{\sigma_v}{v} = \left(\frac{\pi\omega_x^2\omega_y vhc}{2P\sigma\Omega\eta\lambda}\right)^{\frac{1}{2}}\frac{\left[\exp\left\{\frac{2y_1^2}{\omega_y^2}\right\}+\exp\left\{\frac{2[y_1+d\tan\theta]^2}{\omega_y^2}\right\}\right]^{\frac{1}{2}}}{d'\,\beta\tau\exp\left\{-\frac{\beta^2\tau^2}{4}\right\}} \quad (7)$$

$$\beta = \frac{2v}{\omega_x},\quad d' = d-\frac{\omega_x^2}{\omega_y}\theta \quad (8)$$

where the characteristic time interval Δt for the detection process is approximated by ω_x/v, β is an inverse characteristic spot transit time for a particle, proportional to the amount of spot overlap, and d' is a geometrical correction for the actual distance travelled by a particle traversing the spot pairs at angle θ to the axis of the elliptical spots. The geometrical correction reduces to the 2-Spot case for $\omega_x = \omega_y$. The systematic error for the measurement volume geometry given in figure 1 is negligible, where $\omega_y = 5\omega_x$.

Figure 3 shows the uncertainty in measured velocity computed as a function of the spot overlap for two cases; noise dominated and signal dominated. The values given for the parameters in equation 1 are used, with $y_1 = 0$ and $\theta = 0$. Both curves exhibit a minimum, corresponding to the optimal spot overlap. The optimal spot overlap from the Cramer-Rao lower bound is based on the signal to noise characteristics of the detected light, and hence, serves as a figure of merit for the optimal overlap. From a strictly signal processing standpoint, the minimum measurement error is obtained in estimating the peak position when the slope of the bipolar curve is maximized ($\beta\tau$=1). One would expect the measurement error to increase steeply as the slope of the signal at the zero-cross tended toward zero. The curves in figure 3 reflect this behavior and increase sharply away from the minima for $\beta\tau << 1$ and $\beta\tau >> 1$.

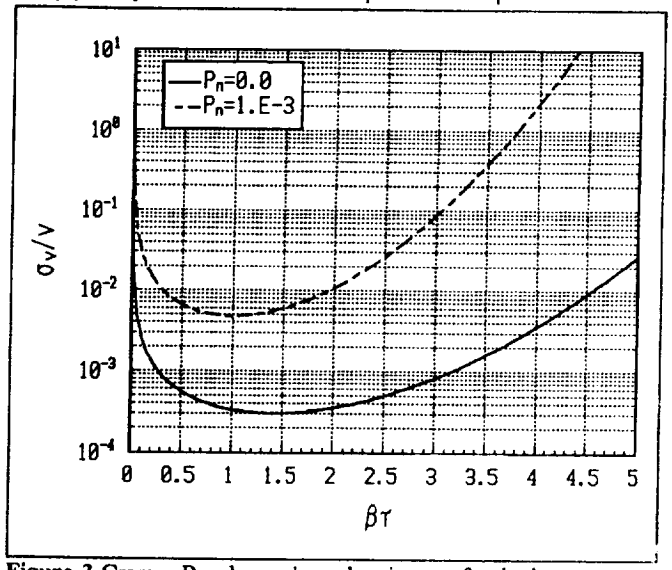

Figure 3 Cramer-Rao lower bound estimate of velocity measurement uncertainty as a function of spot overlap.

For the signal dominated case, the minimum in the measurements error occurs at $\beta\tau$ = 1.4. The optimal spot overlap for the noise dominated case is $\beta\tau$=1, which agrees with the result obtained by Lading (1983). By letting the product

$\beta\tau=1.4$, equation 5 simplifies to:

$$\frac{\sigma_v}{v}=\left(\frac{\pi\omega_x^2\omega_y\nu hc}{\sqrt{2}P\sigma\Omega\eta\lambda}\right)^{\frac{1}{2}}\frac{\left[\exp\left\{\frac{2y_1^2}{\omega_y^2}\right\}+\exp\left\{\frac{2[y_1+d\tan\theta]^2}{\omega_y^2}\right\}\right]^{\frac{1}{2}}}{\left(d-\frac{\omega_x^2}{\omega_y}\theta\right)} \quad (9)$$

Equation 9 can be used as a figure of merit of the performance of a 4-Spot laser anemometer. The effect of particle size, laser power, collection optics, etc; on the measurement error are easily computed. The exponential terms involving y_1 include the effects of the particle trajectory through the probe volume.

Signal Processing Electronics The four raw PMT signals are fed through preamplifiers and low pass filtered before processing. A custom signal processing module was designed and constructed to replace the input conditioning module in a standard TSI model 1990 LFA signal processor. The signal processor uses a comparator circuit to detect the zero-cross of the bipolar signals and Fairchild Advanced Schottky Technology (FAST) TTL logic. The existence of a pulse is first established via a preset threshold level, then the time order of the pulses is verified. The signal processor generates start and stop pulses signaling the beginning and conclusion of a particle transit. The TSI timer module measures the start to stop particle time-of-flight to 1 nsec resolution. The processor determines which spot pair initiates the timer, and hence, the flow direction. A sign bit indicating the flow direction is inserted in the digital word transferred from the counter processor to the host computer. The TSI timer module was modified to insert the sign bit as the 11th bit of the mantissa and to disable other features specific to LFA applications. No additional hardware was added to the module.

The signal processing system design was selected such that an existing LFA data acquisition software package with real time display capability could be employed (Strazisar 1992). The characteristics of the TOFA laser anemometer are transparent to the data acquisition system. Individual particle transit times are recorded with imbedded flow direction. The transit times are converted to velocity, yielding Gaussian velocity pdfs. Since the individual particle velocities are recorded, not a histogram or correlogram of the transit times $\hat{t}$ at probe volume angular orientation $\hat{\alpha}$, non-linear transformations from $\hat{t}$, $\hat{\alpha}$ space to v_x, v_y are not required (Schodl 1986, Mayo *et al.* 1979).

A Microvax II is used to control all of the data acquisition and remote positioning systems. A Macrodyne LVABI is used to record the measured particle transit times and the circumferential shaft position from a commercial encoder. The encoder is programmed to resolve 3000 counts per revolution, yielding 200 location bins per main blade passage in the centrifugal impeller and 100 bins per splitter blade passage. Each time a velocity is measured the LVABI strobes the encoder to provide the shaft circumferential position. For a more detailed description of the shaft angle encoding scheme, see Strazisar *et al.* (1989).

The digital shaft angle encoder is driven by a once-per-rev signal pickup on the rotor drive shaft. The pickup sensor is located 60 cm from the rotor. The encoder can also be programmed to produce a once-per-blade signal; however, the windup or twist in the shaft causes a significant phase shift (5%) between the true blade positions and the generated pulse train. A more stable once-per-blade signal is required to facilitate accurate blade blanking.

The TOFA system normal output signals are pulses, which look very similar to those produced when a blade passes through the probe volume. The blade flash pulses are misinterpreted by the signal processor as data. The processor must be inhibited during the blade flash to eliminate spurious data. Since a reliable once-per-blade signal was not available, the PMT signals themselves were used to generate the once-per-blade inhibit pulses. While this is not the optimum means of generating a blanking signal, it is effective. The price paid is the saturation recovery time of the PMT, which is nominally about 5 μsec at 100% speed where the blade-to-blade period is 200 μsec. The average current level out of the PMTs remains below the damage threshold of 100 μamps.

A separate comparator circuit with its threshold level is used to detect the occurrence of the blade pulse from one of the PMT signals. The blade pulse threshold level is independent of the signal processing threshold level. The i^{th} detected blade pulse is used to generate the i^{th}+1 blade blanking pulse. The intra-blade period and the blade blanking pulse duration are both set by front panel potentiometers on the signal processor. Once tripped, the blade detection comparator is disabled until the intra-blade period time-out expires. The blade blanking circuitry is housed within the signal processor. The PMT signal and the blade blanking pulse are monitored to ensure accurate blanking. The stability of the blade blanking pulse train relative to the true blade position is better than 200 nsec.

Data Acquisition The velocity measurements are resolved by the shaft angle encoder to the circumferential shaft position. The measured velocities in all of the blade passages are combined to build 200 separate histograms across a single blade passage (Hathaway *et al.* 1992). Each histogram is used to compute the mean velocity via a non-linear least squares fit to a Gaussian distribution. Three data sets are acquired at each measurement station at three angular orientations of the probe volume. The angles are nominally oriented at 0° and ±15° to the estimated true flow angle. The computed mean velocities and angular orientations of the probe volume are used in another non-linear least squares fit to determine the velocity vector magnitude $\bar{V}$ and flow angle α:

$$V_j=\bar{V}\cdot\cos[\gamma_j-\alpha] \quad (10)$$

where V_j is the measured mean velocity at spot orientation γ_j.

Positioning System The laser anemometer system was mounted on a 3-axis remotely controlled positioning system. A serial interface connection to the Microvax II computer provides the positioning signals. The goniometric stages for the image rotator and final turning mirror are also connected to the host computer via a serial connection.

Seeding System The flow field was seeded with Polystyrene Latex Spheres (PSL), which are manufactured using the technique developed by Nichols (1987). The nominal 0.7 μm diameter particles were suspended in a concentrated aqueous dispersion. The seed suspension was diluted with ethanol and the mixture was injected into the flow stream using a commercial paint spraying air nozzle, approximately 5 m upstream from the rotor. The ethanol evaporated by the time the seed reached the rotor leading edge.

CENTRIFUGAL COMPRESSOR FACILITY

The compressor that is the subject of investigation, using the 4-Spot TOFA, is a 4.5 kg/sec, 4:1 pressure ratio centrifugal compressor. The impeller has 15 main blades and 15 splitter blades with 50° of back-sweep at the exit. The design rotational speed is 21789 rpm, which results in a maximum blade passing

frequency of 10.9 kHz in the splitter region. Blade heights range from 64 mm at the inlet to 17 mm at the exit. The inlet and exit tip diameters are 210 mm and 431 mm, respectively. The impeller is being tested with a vaneless diffuser in order to duplicate the environment that was used in a 3-D steady viscous code analysis.

Optical access is provided by windows placed at 16 locations along the compressor flow path. The window surfaces were kept flat in order to prevent optical distortion of the laser beams passing through them. Several very small windows were used in order to keep deviations from the true shroud contour, caused by the flat window surface, to a minimum as well. Circular windows are used in areas where shroud curvature is high and range in size from 14 to 23 mm in diameter. Rectangular windows are used upstream of the impeller and circular arc windows are used downstream. These windows can be slightly larger because there is less shroud curvature in either the streamwise or circumferential directions, or both. The window shapes and dimensions that were selected result in maximum mismatch of 203 to 381 μm between the window surfaces and the true shroud contour.

The sixteen individual windows are epoxied into eight window frames that are then installed along the compressor flow path in pairs. Each frame contains from one to three separate windows, so that a particular pair of frames will provide optical access to anywhere from three to five locations along the flow path. Several combinations of window frame pairs are required in order to obtain access to all 16 measurement stations. Figure 4 shows one combination that contains a total of five windows labeled 1-A, 1-C, 3-A, 3-C, and 3-E.

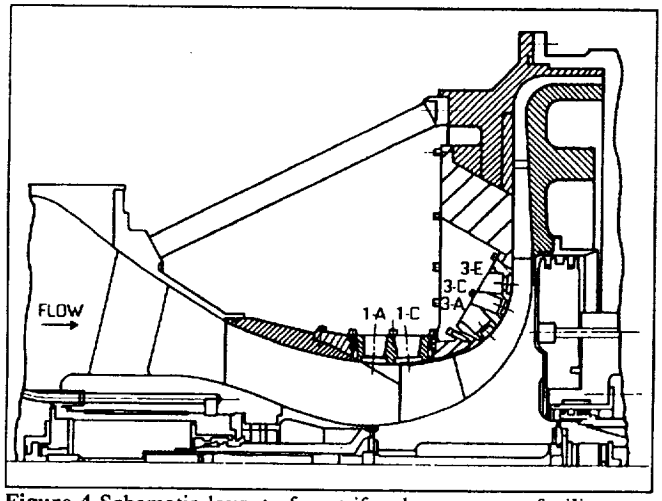

Figure 4 Schematic layout of centrifugal compressor facility showing one configuration of window inserts

EXPERIMENTAL RESULTS

The rotor was gradually ramped up to speed and allowed to warm up. After steady state operation was achieved, the exit clearance gap was closed to 400 μm, which is larger than the design spacing of 200 μm. The mass flow through the rotor was 5 kg/s with the throttle valve fully open at 100% speed, or 21789 RPM corrected speed.

The laser anemometer system was positioned to window station 3-C. Measurements have been obtained in all 5 of the windows; however, only measurements within the splitter region are shown here. The blade blanking pulses were matched to the blade frequency. In the splitter region, approximately 25% of the bins were blanked due to blade flash. Approximately 50,000

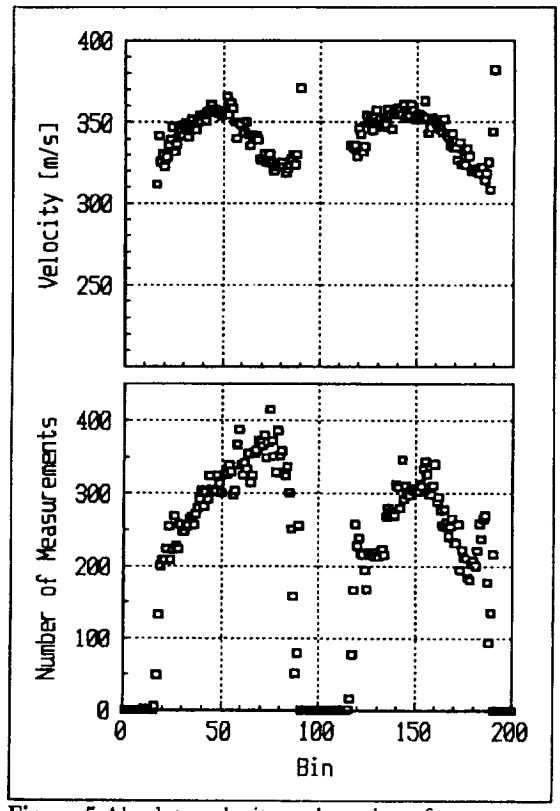

Figure 5 Absolute velocity and number of measurements per bin across the blade pitch.

velocity measurements were recorded at each probe volume orientation. The data were averaged across all of the passages to produce a single blade pitch velocity profile. The average number of measurements per bin was 300. A sample velocity profile and number of measurements per bin across the blade pitch are shown in figure 5. The suction and pressure surfaces of the blades are located at bins 10,110 and 91,191 respectively. The total number of measurements was 51896. The average rms deviation in the measurements is approximately 15%. Most of the deviation is from the flow turbulence, a small portion may be due to the passage-to-passage averaging of the data. The data rate varied across the blade pitch. In most instances the pressure surface side of the blades had a higher data rate than the suction side.

The blade passage velocity survey shown in figure 6 was taken starting at 75% span, decreasing in 12.5% span increments, down to 12.5% span. 100% span corresponds to the shroud location. A total of six span positions are shown. Three probe volume angular orientations were used at each position. The velocity data shown are absolute velocity magnitudes. The approximate blade shapes are evident from the blanking intervals. The blades are thickest at the hub and thinnest at the shroud. The data rate across the blade span varied from 2 KHz down to 300 Hz. The velocity data obtained are not meant to show the true impeller performance since they were not obtained at operating conditions of interest. The data does show that the 4-Spot TOFA is a capable system for obtaining measurements in the complex flow fields anticipated in a centrifugal impeller. The profiles show that the flow through the splitter blade rows is not identical under these conditions.

The data rate gradually decreased as the run progressed. Seed material slowly built up on the window ports until the data rate fell to an unacceptably low level. The low data rate (300 Hz) was due to seed build up, and did not correspond to a degradation in the instrument performance, or lack of seed. In

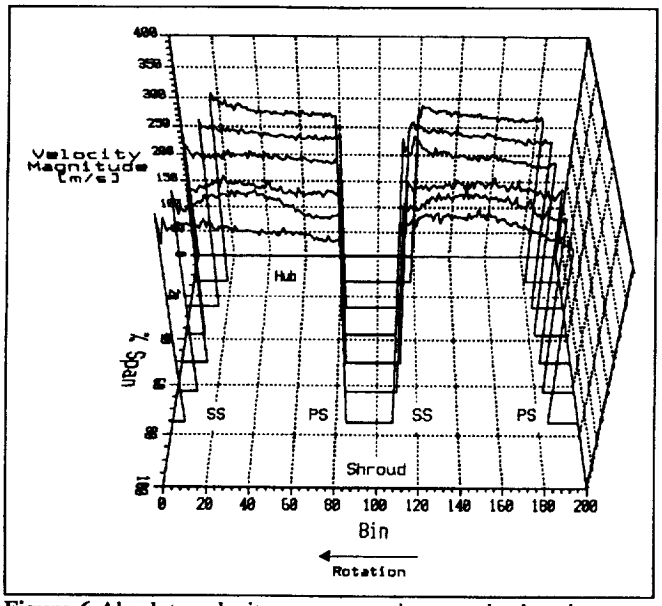

Figure 6 Absolute velocity surveys at six spanwise locations.

these preliminary velocity surveys, the clearance gap has not been closed down in order to avoid accidental damage to the rotor housing. The large tip clearance may be causing gross tip clearance flows which may be depositing seed material on the windows. We are currently investigating the source of the material build up and possible remedies.

No attempt has been made to optimize the flare light rejection capabilities of the 4-Spot system. Spatial filtering techniques are readily employed to reduce surface flare light from reaching the detector (Seasholtz *et al.* 1984). Also, measurements closer to the blade tips can be obtained by tilting the axis of the spots slightly relative to the blades, or by using an externally supplied once-per-blade signal.

CONCLUSIONS

A novel laser anemometer system has been described which is well suited for the environment encountered in centrifugal compressor facilities. The wide range of anticipated velocities (160-700 m/s) are easily accommodated by the 4-Spot TOFA. Accurate blade blanking was obtained by using the PMT signals directly. The signal processing hardware has been designed to simplify system integration into existing facilities equipped with LFA signal processing equipment. Preliminary velocity surveys show that the instrument is capable of obtaining measurements in the small blade passages of a centrifugal compressor, including the splitter region.

ACKNOWLEDGEMENTS

The authors would like to thank W. Trevor John and Michael Krasowski for their diligent efforts in the development of the signal processing electronics. The advice and expertise of Tony Strazisar proved invaluable in simplifying the data acquisition and processing. The efforts of Richard Brokopp, Theresa Gibson, Robert Gronski, and Kevin McCormick in maintaining and operating the compressor facility are greatly appreciated.

REFERENCES

Ahmed, N. A. and Elder, R. L., 1990, "Flow Investigation in a Small High Speed Impeller Passage Using Laser Anemometry," ASME Paper 90-GT-233.

Brokopp, R. A. and Gronski, R. S., 1992, "Small Engine Test Facility Compressor Testing Cell at NASA Lewis Research Center,", NASA TM-105685.

Elder, R. L., Foster, C. P., and Gill, M. E., 1986, "Application of Doppler and Transit Laser Anemometry in Small Turbomachines," AGARD CP-33.

Hathaway, M. D., Chriss, R. M., Wood, J. R., and Strazisar, A. J., 1992, "Experimental and Computational Investigation of the NASA Low-Speed Centrifugal Compressor Flow Field," 37th ASME International Gas Turbine Conference, Cologne, Germany.

Krain, H., 1988, "Swirling Impeller Flow" ASME Journal of Turbomachinery, Vol. 110, pp. 122-128.

Lading, L., 1983, "Estimating Time and Time-Lag in Time-of-Flight Velocimetry," Appl. Opt., Vol. 22, No. 22, pp. 3637-3643.

Lading, L., and Jensen, A. S., 1980, "Estimating The Spectral Width of a Narrowband Optical Signal," Appl. Opt., Vol. 19, No. 16, pp. 2750-2756.

Jensen, A. S., 1977, "Optimum Strategies of Parameter Estimation For a Poisson-Distributed Signal," Risø National Laboratory Report M-1959 Roskilde, Denmark.

Mayo, W. T., Smart, A., E., and Hunt, T. E., 1979, "Laser Transit Anemometer With Microcomputer and Special Digital Electronics: Measurements in Supersonic Flows," ICIASF Record pp. 146-153.

Nichols, C. E., Jr., "1987, "Preparation of Polystyrene Microspheres for Laser Velocimetry in Wind Tunnels," NASA TM 89163.

Schodl, R., 1986, "Laser-Two-Focus Velocimetry," AGARD-CP-399, Paper 7.

Schodl, R., 1989, "A New Multi-Colour Laser Two Focus Velocimeter for 3-Dimensional Flow Analysis," ICIASF Record, pp.142-151.

Seasholtz, R. G., Oberle, L. G., and Weikle, D. H., 1984, "Optimization of Fringe-Type Laser Anemometers for Turbine Engine Component Testing," AIAA-84-1459.

Strazisar, A. J., Wood, J. R., Hathaway, M. D., and Suder, K., L., 1989, "Laser Anemometer Measurements in a Transonic Axial-Flow Fan Rotor," NASA TP-2879.

Strazisar, A. J., 1992, "Laser Anemometry Data Acquisition and Reduction Software (LADARS)," NASA Internal publication.

Wernet, M. P., and Edwards, R. V., 1986, "Implementation of a New Type of Time-of-Flight Laser Anemometer," Appl. Opt., Vol. 25, No. 5., pp. 644-648.

Wernet, M. P., and Oberle, L. O., 1987, "Laser Anemometry for Turbine Applications," ASME Paper 87-GT-241.

Whalen, A. D., 1971, "Detection of Signals in Noise," Academic, New York, pp. 337-339.

REPORT DOCUMENTATION PAGE

Form Approved
OMB No. 0704-0188

1. AGENCY USE ONLY (*Leave blank*)	2. REPORT DATE	3. REPORT TYPE AND DATES COVERED
	July 1992	Technical Memorandum

4. TITLE AND SUBTITLE

A 4-Spot Time-of-Flight Anemometer for Small Centrifugal Compressor Velocity Measurements

5. FUNDING NUMBERS

WU–505–62–50
1L162211A47A

6. AUTHOR(S)

Mark P. Wernet and Gary J. Skoch

7. PERFORMING ORGANIZATION NAME(S) AND ADDRESS(ES)

NASA Lewis Research Center
Cleveland, Ohio 44135–3191
and
Propulsion Directorate
U.S. Army Aviation Systems Command
Cleveland, Ohio 44135–3191

8. PERFORMING ORGANIZATION REPORT NUMBER

E–7112

9. SPONSORING/MONITORING AGENCY NAMES(S) AND ADDRESS(ES)

National Aeronautics and Space Administration
Washington, D.C. 20546–0001
and
U.S. Army Aviation Systems Command
St. Louis, Mo. 63120–1798

10. SPONSORING/MONITORING AGENCY REPORT NUMBER

NASA TM–105717
AVSCOM TR–92–C–026

11. SUPPLEMENTARY NOTES

Prepared for the Sixth International Symposium on the Application of Laser Techniques to Fluid Mechanics sponsored by the Instituto Superio Téchico, Lisbon, Portugal. July 20–23, 1992. Mark P. Wernet, NASA Lewis Research Center, Cleveland, Ohio, and Gary J. Skoch, Propulsion Directorate, U.S. Army Aviation Systems Command, Lewis Research Center, Cleveland, Ohio. Responsible person, Mark P. Wernet, (216) 433–3752.

12a. DISTRIBUTION/AVAILABILITY STATEMENT

Unclassified–Unlimited
Subject Category 35

12b. DISTRIBUTION CODE

13. ABSTRACT ***(Maximum 200 words)***

The application of laser anemometry techniques in turbomachinery facilities is a challenging dilemma requiring an anemometer system with special qualities. In this work we describe the use of a novel laser anemometry technique applied to a small 4.5 kg/s, 4:1 pressure ratio centrifugal compressor. Sample velocity profiles across the blade pitch are presented for a single location along the rotor. The results of the intra-blade passage velocity measurements will ultimately be used to verify CFD 3-D viscous code predictions.

14. SUBJECT TERMS

Laser anemometers; Centrifugal compressors

15. NUMBER OF PAGES

8

16. PRICE CODE

A02

17. SECURITY CLASSIFICATION OF REPORT	18. SECURITY CLASSIFICATION OF THIS PAGE	19. SECURITY CLASSIFICATION OF ABSTRACT	20. LIMITATION OF ABSTRACT
Unclassified	Unclassified	Unclassified	